Whole-body biomechanical load in running-based sports

Verheul, J.; Gregson, Warren; Lisboa, Paulo; Vanrenterghem, Jos; Robinson, Mark A.

Link to publication on Research at Birmingham portal

1   **Whole-body biomechanical load in running-based sports: the validity of**

2   **estimating ground reaction forces from segmental accelerations**

3

4   **Original research article**

5

6   **Authors**:

7   Jasper Verheul[1], Warren Gregson[1], Paulo Lisboa[2], Jos Vanrenterghem[3], Mark A. Robinson[1]

8   1. Research Institute for Sport and Exercise Sciences, Liverpool John Moores University,

9   Liverpool, United Kingdom

10   2. Department of Applied Mathematics, Liverpool John Moores University, Liverpool, United

11   Kingdom

12   3. Faculty of Kinesiology and Rehabilitation Sciences, KU Leuven, Leuven, Belgium

13

14   **Corresponding Author**:

15   Jasper Verheul (J.P.Verheul@2016.ljmu.ac.uk)

16   Research Institute for Sport and Exercise Sciences, Liverpool John Moores University

17   Tom Reilly Building, Byrom Street, L3 5AF, Liverpool, United Kingdom

18

19   **Abstract word count**: 250

20   **Text-only word count**: 3519

21   **Number of figures and tables**: 2 figures and 1 table

22

23

24 **Whole-body biomechanical load in running-based sports: the validity of**

25 **estimating ground reaction forces from segmental accelerations**

26

27 **Abstract**

28 *Objective:* Unlike physiological loads, the biomechanical loads of training in running-based sports are

29 still largely unexplored. This study, therefore, aimed to assess the validity of estimating ground

30 reaction forces (GRF), as a measure of external whole-body biomechanical loading, from segmental

31 accelerations.

32 *Methods:* Fifteen team-sport athletes performed accelerations, decelerations, 90° cuts and straight

33 running at different speeds including sprinting. Full-body kinematics and GRF were recorded with a

34 three-dimensional motion capture system and a single force platform respectively. GRF profiles were

35 estimated as the sum of the product of all fifteen segmental masses and accelerations, or a reduced

36 number of segments.

37 *Results*: Errors for GRF profiles estimated from fifteen segmental accelerations were low (1-2 N·kg^{-1})

38 for low-speed running, moderate (2-3 N·kg^{-1}) for accelerations, 90° cuts and moderate-speed running,

39 but very high (>4 N·kg^{-1}) for decelerations and high-speed running. Similarly, impulse (2.3-11.1%),

40 impact peak (9.2-28.5%) and loading rate (20.1-42.8%) errors varied across tasks. Moreover, mean

41 errors increased from 3.26±1.72 N·kg^{-1} to 6.76±3.62 N·kg^{-1} across tasks when the number of segments

42 was reduced.

43 *Conclusions:* Accuracy of estimated GRF profiles and loading characteristics was dependent on task,

44 and errors substantially increased when the number of segments was reduced. Using a direct

45 mechanical approach to estimate GRF from segmental accelerations is thus unlikely to be a valid

46 method to assess whole-body biomechanical loading across different dynamic and high-intensity

47 activities. Researchers and practitioners should, therefore, be very cautious when interpreting

48 accelerations from one or several segments, as these are unlikely to accurately represent external

49 whole-body biomechanical loads.

52

Introduction

Training loads are monitored in sports as part of a process which aims to enhance performance, whilst simultaneously reducing the risk of injury. Although physiological loads have been investigated extensively, biomechanical load measures are still limited and, therefore, largely unexplored [1]. Based on the assumption that accelerations of the trunk are a good representation of whole-body centre of mass (CoM) accelerations, trunk accelerometry derived load measures (e.g. New Body Load, Dynamic Stress Load, PlayerLoad, Force Load) have been used to quantify and evaluate whole-body biomechanical loads [2–6]. However, evidence relating accelerations of the trunk to established measures of biomechanical loading is yet lacking. In fact, it has been shown that accelerations of individual segments (including the trunk) cannot accurately represent whole-body biomechanical loads [7–11].

Ground reaction forces (GRFs) are a well-established measure of whole-body biomechanical loading. GRFs have been used to optimise sprint performance [12,13], improve running economy [14] and identify or reduce potential injury risk factors [15,16], and might thus be used to further understand the role of external biomechanical forces in performance enhancement and injury prevention. Moreover, GRF drives internal force production and contributes to internal stresses on e.g. muscles, tendons and bones [17,18], which are currently difficult to measure in the field [1]. Since these structure- or tissue-specific loads are the primary cause of e.g. overuse injuries [19], monitoring GRF in the field would be a first step towards investigating internal biomechanical loads in more detail. However, valid methods for accurately estimating GRF outside laboratory settings are currently unavailable.

Body-worn sensors, such as accelerometers, are commonly used in sports to measure and monitor numerous training load related metrics [20,21]. Given their widespread application to measure accelerations of various body segments [22,23], accelerometers might be used to estimate GRF, which can be defined as the sum of the product of segmental mass and CoM accelerations of all body segments. This alternative expression of Newton's second law provides a way by which the contribution of multiple segmental accelerations to the GRF can be systematically examined, especially since accelerations of the trunk or other individual segments have been shown to not be sufficient to estimate GRF for several straight running and cutting activities [7–9,11,24]. Other studies have indeed

4

80 shown that for constant speed running, GRF can be estimated from seven [25] or eleven [26] segmental

81 accelerations measured with a laboratory based motion capture system. However, it is unknown

82 whether GRF for dynamic and high-intensity activities frequently undertaken in running-based sports

83 (e.g. rapidly accelerating, decelerating, cutting, sprinting) can be accurately estimated from segmental

84 accelerations and/or what the minimal required number of segments is.

85 If simultaneously measured segmental accelerations can be used to estimate GRF, this might

86 eventually allow GRF to be estimated in field settings and provide a meaningful measure of external

87 whole-body biomechanical loading. The aim of this study was, therefore, 1) to investigate whether

88 segmental accelerations measured in a laboratory setting can be used to estimate GRF for a variety of

89 dynamic and high-intensity tasks typically performed during running-based (team-) sports, and 2) to

90 determine the minimal number of segments required.

91 **Methods**

92   *Participants*. Fifteen team-sports athletes participated in this study (12 males and 3 females,

93 age 23±4 yrs, height 178±9 cm, body mass 73±10 kg). All participants were healthy and physically

94 active for at least three hours per week (sports participation 7±5 hrs per wk). This study was approved

95 by the Liverpool John Moores University ethics committee and participants provided informed

96 consent according to the ethics regulations.

97   *Protocol*. After a standardised warm-up, participants performed a range of dynamic and high-

98 intensity running tasks including accelerations, decelerations, cutting, and steady running at constant

99 speeds ranging from 2 m·s^{-1} to maximal sprinting (~7 m·s^{-1}, individual specific). Participants were

100 instructed to land with one whole foot on a single force platform embedded in the ground and

101 performed a minimum of five trials for each leg per task. For acceleration trials, participants were

102 instructed to accelerate from stand-still to their maximal sprinting speed (achieved in ~20 m), while

103 landing on the force platform for their second or third step of accelerating. For decelerations,

104 participants were instructed to decelerate as quickly as possible from maximal sprinting to immediate

105 stand-still, while landing on the force platform for their first or second step of decelerating. Cutting

106 trials were performed as a sharp change of direction on the force platform at a 90° angle from the

107 straight running direction. Steady (straight) running trials were performed at a constant low (2-3 m·s^{-1}),

108 ^{1}), moderate (4-5 m·s^{-1}) or high running speed (>6 m·s^{-1}), including maximal sprinting. Running

109 speeds were measured with photocell timing gates (Brower Timing Systems, Draper, UT, USA) and

110 controlled by giving verbal feedback to speed up or slow down after each trial. Only trials within a ±

111 5% range of the target speed were included.

112   *Kinematic and kinetic data collection*. During the trials, full-body kinematic data were

113 collected using a seventy-six retro-reflective marker set attached to anatomical landmarks of the body

114 (appendix A). Three-dimensional kinematic and kinetic data were synchronously recorded with ten

115 infrared cameras (Qqus 300+, Qualisys Inc., Gothenburg, Sweden) sampling at 250 Hz, in

116 combination with a single force platform (9287B, 90x60 cm, Kistler Holding AG, Winterthur,

117 Switzerland) embedded in the ground, sampling at 3000 Hz. Marker positions and ground reaction

118 forces (GRF) were recorded, synchronised and tracked using Qualisys Track Manager Software (QTM

119 version 2.16, Qualisys Inc., Gothenberg, Sweden). A static calibration was recorded at the start of each

120 session to determine the local coordinate systems, joint centres and segment dimensions for each

121 participant. From the marker data, a fifteen segment (head, trunk, pelvis, upper arms, forearms, hands,

122 thighs, shanks and feet) six-degree-of-freedom model was built, with segment mass and inertial

123 properties based on Dempster's regression equations [27] and represented as geometric volumes [28].

124 Kinematic and kinetic data were exported to Visual3D (C-motion, Germantown, MD, USA) and

125 Matlab (version R2017b, The MathWorks, Inc., Natick, MA, USA) for further processing and

126 analysis.

127   *Data processing and analysis*. Marker trajectories and force platform data were filtered with a

128 2nd order Butterworth low-pass filter with 20 Hz and 50 Hz cut-off frequencies respectively. Trunk

129 defining marker trajectories were, however, filtered at 10 Hz based on a sensitivity analysis for

130 optimal GRF prediction (appendix B). For each trial, touch-down and take-off from the force platform

131 were identified by a 20 N threshold of the vertical GRF and resultant GRF was calculated from the

132 three individual force components (F_x, F_y, F_z). The centre of mass (CoM) position for each segment

133 was used to define segmental movements from which accelerations were calculated as the double

134   differentiation (using three-point derivatives) of CoM motion along the three axes of the lab (x-y-z).

135   Resultant GRF curves were then estimated as the sum of the product of each segmental mass and CoM

136   acceleration in the three directions, according to equation 1.

$$GRF_{res,estimated} = \sqrt{\left(\sum_{n=1}^{1,2,3,...15}(a_{n,x} \cdot m_n)\right)^2 + \left(\sum_{n=1}^{1,2,3,...15}(a_{n,y} \cdot m_n)\right)^2 + \left(\sum_{n=1}^{1,2,3,...15}(a_{n,z} \cdot m_n)\right)^2} \qquad \text{Eq. 1}$$

137   In which a is the segmental acceleration, m the segmental mass and n the number of segments

138   included. To determine the number of segments required to accurately estimate resultant GRF, all

139   different segment combinations to estimate GRF from were examined. A total of 32,676 unique

140   combinations were analysed with a minimum of one and a maximum of fifteen segments. To ensure a

141   constant total body mass, masses of the segments not included in a specific combination were equally

142   divided and added to the segmental masses that were part of that combination.

143   Measured and estimated GRF curves were normalised to each participant's body mass. Accuracy of

144   estimated GRF profiles was evaluated by the absolute and relative curve root mean square errors

145   (RMSE). In addition, the accuracy of estimated GRF loading characteristics impulse (area under the

146   GRF curve), impact peak (force peak during the first 30% of stance) and loading rate (average GRF

147   gradient from touch-down to impact peak) was calculated and assessed. RMSE was rated as very low

148   (<1 N·kg^{-1}), low (1-2 N·kg^{-1}), moderate (2-3 N·kg^{-1}), high (3-4 N·kg^{-1}) or very high (>4 N·kg^{-1}).

149   RMSE values were analysed for all possible combinations of segments per task, as well as all trials

150   combined, to determine the best combination (i.e. lowest mean RMSE across trials) for each number

151   of segments. Estimated GRF loading characteristics errors were rated as very low ($<5\%$), low (5-

152   10%), moderate (10-15%), high (15-20%) or very high ($>20\%$), which was based on meaningful

153   performance or injury related differences in GRF [12,13,15]. Moreover, linear regression analyses were

154   performed between GRF loading characteristics (impulse, impact peak, loading rate) derived from the

155   estimated and measured GRF profiles. Regressions were performed per task, as well as for all trials

156   combined to examine the generalisability of GRF estimations across tasks, and rated as very weak

157   ($R^2<0.1$), weak (R^2=0.1-0.3), moderate (R^2=0.3-0.5), strong (R^2=0.5-0.7), very strong (R^2=0.7-0.9) or

158   extremely strong (R^2=0.9-1) [29]. Furthermore, Bland-Altman analyses [30] were performed across tasks to

159　explore mean differences and 95% limits of agreement between the estimated and measured GRF

160　loading characteristics.

161　**Results**

162　　　*Full body segmental accelerations*. Accuracy of estimated GRF profiles from fifteen

163　segmental accelerations (full-body) varied across tasks (figure 1; table 1). Overall curve errors

164　(RMSE) were low for running at low speeds (2-3 $m·s^{-1}$) and moderate for accelerations, 90° cuts and

165　moderate-speed (4-5 $m·s^{-1}$) running. However, mean RMSE was very high for decelerations and high-

166　speed running (>6 $m·s^{-1}$).

167　The accuracy of estimated GRF loading characteristics varied between metrics and was dependent on

168　task (table 1). Impulses were accurately estimated with very low errors for 90° cuts and running at

169　constant low and moderate speeds, low errors for accelerations, and moderate errors for decelerations

170　and high-speed running. Similarly, impact peaks were estimated with low to moderate (9.2-15%)

171　errors for all tasks, except accelerations, which had very high (28.5%) impact peak errors. Loading

172　rate errors however, were very high (20.1-42.8%) across all tasks.

173　Correlations and agreement between measured and estimated GRF loading characteristics across all

174　tasks varied. Impulses had extremely strong correlations, with a small bias and 95% confidence

175　interval of the limits of agreement (-0.04 to 0.45 $N·s·kg^{-1}$) (figure C.1 A and D; table 1). Despite the

176　very strong correlation and small bias for impact peaks however, there was a large variation of the

177　differences with limits of agreement ranging from -12.6 to 8.4 $N·kg^{-1}$ (figure C.1 B and E).

178　Furthermore, measured and estimated loading rates had a strong correlation ($R^2 = 0.68$), but a large

179　bias and limits of agreement (-985 to 397 $N·kg^{-1}·s^{-1}$) (figure C.1 C and F).

180　　　*Segment reductions*. The best combinations of segments across all tasks for each given

181　number of segments are shown in table C.1. GRF estimated from a single segment was the best across

182　tasks from trunk accelerations, despite mean RMSE being very high. Furthermore, the trunk was part

183　of all combinations of segments, and thus the main contributor to GRF, followed by the thighs, head,

184　shanks, arms, pelvis and feet (in descending order of importance).

8

185   Reducing the number of segmental accelerations to estimate GRF substantially increased errors for all

186   tasks (figure 2). To achieve estimated GRF errors that were moderate or better (<3 N·kg^{-1}) for at least

187   50% of the combinations and trials, a minimum of two and three segments was required for low- and

188   moderate-speed running respectively, but eight (90° cuts) and eleven (accelerations) for more dynamic

189   tasks. Moreover, for the high-intensity tasks (decelerations and high-speed running) the majority of

190   trials and combinations resulted in very high errors, regardless of the number of segment used (figure

191   2).

192   **Discussion**

193   *Estimating GRF from full-body segmental accelerations*. The main aim of this study was to

194   assess the validity of estimating ground reaction forces (GRF) from segmental accelerations for a

195   range of dynamic and high-intensity running tasks typically performed during running-based sports.

196   From all fifteen body segments, overall GRF profiles as well as specific loading characteristics were

197   estimated with varying accuracy. Overall loading errors (RMSE and impulse) for example, were

198   considerably lower for running at low and moderate speeds (~2-5%) compared to the higher intensity

199   tasks (e.g. decelerations, high-speed running) (~6-12%). Similarly, impact peak and loading rate errors

200   ranged from ~9% for the lower intensity tasks to >40% for higher intensity tasks (figure C.1 E and F).

201   Meaningful performance or injury related differences in loading characteristics can, however, be as

202   small as ~3-10% [12,13,15]. Errors of the magnitude observed in this study could thus already rule out

203   certain applications of monitoring GRF estimated from full-body segmental accelerations. Using a

204   direct mechanical approach to estimate GRF from full-body segmental accelerations might, therefore,

205   not be a valid method to assess whole-body biomechanical loading for dynamic and high-intensity

206   activities. Consequently, future research should investigate if segmental accelerations might be used to

207   assess more specific measures of biomechanical loading (e.g. internal structural loads).

208   Estimated GRF results in this study are comparable to other laboratory-based studies aiming to predict

209   GRF from marker trajectory data using a mechanical approach. The impulse errors for low-speed

210   running (2.3%), impact peak errors for moderate-speed running (9.2%) and correlations between

211   estimated and measured impact peaks for low- to high-speed running (R^2=0.77-0.96) found in the

9

212 current study are similar to results reported in previous studies that aimed to predict GRF from marker

213 trajectory data for comparable constant speed running tasks [25,26,31]. However, this study extends

214 beyond other studies in that similar results were also achieved for a range of high-intensity and

215 dynamic running tasks frequently undertaken in running-based sports. Moreover, previous studies

216 failed to include the mediolateral and anteroposterior components of acceleration and GRF [25,31],

217 utilised small sample sizes [25,26,31] and/or investigated running on a treadmill rather than overground

218 [26,31], all of which limit their ability to translate their findings from the lab to an applied sport setting.

219 In most running-based sports, the dynamic and high-intensity movements examined in this study are

220 regularly performed [32–34]. The musculoskeletal demands of these tasks are high [35–37] and thus comprise

221 a large amount of the total biomechanical loads experienced during training and competition.

222 Therefore, highly accurate estimates of GRF loading characteristics across different tasks (including

223 decelerations and running at high speeds) are essential to explore and understand the biomechanical

224 demands of training in greater detail. As discussed above however, the loading characteristics errors

225 observed in this study might already rule out several performance and injury related applications of

226 monitoring GRF. Future work could, therefore, investigate if the strong to extremely strong

227 correlations between estimated and measured GRF characteristics found in this study (figure C1; table

228 1) can be used to recalculate and improve the estimated loading characteristics, to quantify the

229 biomechanical stresses of training more accurately.

230   *Segment reductions*. Full-body wireless accelerometry suits have been shown to be a reliable

231 and valid method for simultaneously measuring accelerations of all body segments (e.g. Xsens MVN

232 [38]) and have been used to estimate GRF and moments during walking [39]. It is, however, likely to be

233 unpractical to use these systems for load monitoring during training and competition on a day-to-day

234 basis. Therefore, we examined the effects of reducing the number of segments and the minimal

235 number of segments required for acceptable GRF estimates. Although the lower intensity tasks (low-

236 and moderate-speed running) were relatively robust against segment reductions, estimated GRF

237 profiles for the more sport-specific dynamic and high-intensity tasks substantially deteriorated (figure

238 2). When the number of segmental accelerations was reduced to six segments for instance (i.e.

239 excluding the head, arms and feet), errors substantially increased to very high for all tasks (figure 2;

240 table C.1). Previous studies have reported similar findings of considerably decreased accuracy in

241 whole-body CoM estimates (and thus GRF) for constant speed running [7], side cutting [11], and jumping,

242 kicking and throwing [40], when the number of segments was only slightly reduced. Furthermore, the

243 very high errors observed in this study for GRF estimated from one segment (i.e. the trunk) are in line

244 with other studies which reported that individual segmental accelerations cannot be used to accurately

245 estimate GRF for steady running at constant speeds [7,9] and side cutting [8,11]. These findings, together

246 with the present results suggest that estimating GRF from one or several segmental accelerations using

247 a mechanical approach is not a valid method to accurately predict GRF for dynamic and high-intensity

248 running tasks.

249 A crucial requirement for GRF to be used as a meaningful measure of biomechanical loading in the

250 field, is that GRF estimates are highly accurate across different tasks. Since errors of the magnitude

251 observed in this study might already rule out certain applications as discussed above, the increased

252 GRF errors for a reduced number of segments probably further eliminate several aspects that make

253 GRF a meaningful load measure. Consequently, the usefulness of less accurate GRF estimates from a

254 reduced number of segments (and individual segmental accelerations from e.g. the trunk especially) as

255 a measure of biomechanical loading, is questionable. Researchers and practitioners should, therefore,

256 be very cautious when interpreting one or several segmental accelerations (or derived load measures),

257 as these are unlikely to be a valid and meaningful measure of whole-body biomechanical loading.

258 *Alternative methods to assess whole-body biomechanical loading in the field.* Segmental

259 accelerations used to estimate GRF in this study were derived from marker trajectory data recorded

260 with a three-dimensional motion capture system. Similar to force platforms, such systems are not

261 typically available in the field and if they are, data collection is laborious and impractical for

262 immediate analysis on a daily basis. In contrast to force platform and marker-based motion capture

263 technologies however, body-worn accelerometers are commonly used in the field and thus relatively

264 easily accessible [20,21]. Moreover, the use of in-field markerless motion capture systems are currently on

265 the rise as a non-invasive way of quantifying movement in different sports [41–43]. Future research

266   should, therefore, investigate if body-worn (or even implantable [44]) accelerometers or markerless

267   motion capture systems can provide accurate measures of full-body segmental CoM accelerations, to

268   eventually estimate GRF in field settings.

269   This study aimed to estimate GRF from segmental accelerations using a direct mechanical approach.

270   Alternative methods have, however, emerged that use machine learning methods to predict GRF [45–48].

271   For example, neural network approaches have been used successfully to predict GRF from marker

272   trajectory data [46,48] or body-worn accelerometers [45,47] for a variety of running tasks. Despite the

273   promising results, there might be disadvantages of using these computational rather than mechanical

274   approaches to estimate GRF for load monitoring purposes. Computational methods could prevent one

275   from exploring the underlying physical mechanisms of the predicted variable (e.g. GRF, joint

276   moments) which may limit its use for e.g. explaining injury mechanisms or defining performance

277   enhancing criteria. Machine learning could thus offer a powerful alternative for our mechanistic

278   approach, but future research should examine the explanatory ability of these methods for underlying

279   physical mechanisms.

280   *Methodological limitations.* A limitation of the mechanical approach described in this study is

281   that estimated GRF errors are solely due to measurement and methodological inaccuracies. Segmental

282   masses and inertial properties for example, were based on standardised values relative to the total body

283   mass [27] and standardised geometric shapes [28] respectively. Future work could, therefore, investigate

284   how the present results might be improved by using participant-specific properties measured from e.g.

285   a DXA scanner [49,50]. Other factors that could affect the estimated GRF accuracy are soft-tissue

286   artefacts [51] and filter cut-off frequencies [52,53]. For example, impact peak errors increased for higher

287   magnitudes, especially for decelerations (figure 2; table 1). These increased errors are likely due to the

288   considerably higher impacts, and consequent tissue vibrations, of landing for these higher-intensity

289   tasks. A sensitivity analysis of different cut-off filters showed that applying a lower 10 Hz filter to the

290   trunk marker (which typically were more affected due to their attachment to tight-fitting clothing

291   rather than the skin) resulted in the lowest estimated GRF errors across the different tasks (appendix

292   B). Future work should, however, consider the effects of soft-tissue artefact and filter cut-off

293 frequency, as well as the use of different filters for kinematic and kinetic data, when estimating GRF

294 from segmental accelerations.

Conclusions

296 This study showed that accuracy of GRF profiles and loading characteristics estimated from full-body

297 segmental accelerations is dependent on task. Moreover, errors substantially increased when the

298 number of segments was reduced. It is, therefore, unlikely that one or several segmental accelerations

299 can provide valid estimates of GRF for biomechanical load monitoring purposes, using a direct

300 mechanical approach. Researchers and practitioners should, therefore, be very cautious when

301 interpreting accelerations from one or several segments as these are unlikely to accurately represent

302 external whole-body biomechanical loads.

Practical applications

304 • We suggest ground reaction forces (GRF) as a meaningful measure of overall whole-body

305   biomechanical loading, and a first step towards investigating structure-specific internal loads,

306   in running-based sports.

307 • Accuracy of GRF profiles and loading characteristics estimated from fifteen segmental

308   accelerations was dependent on task, with higher accuracy for lower intensity tasks (e.g.

309   running at low speeds). Moreover, errors substantially increased when the number of segments

310   was reduced.

311 • A direct mechanical approach cannot provide valid estimates of GRF from segmental

312   accelerations across dynamic and high-intensity running tasks that are frequently performed

313   during running-based sports.

314 • Acceleration signals and derived training load measures from one or several segments are

315   unlikely to accurately represent whole-body biomechanical loads.

316 • Researchers and practitioners should be very cautious when interpreting accelerations from

317   one or several segments as a measure of external whole-body biomechanical loading.

13

318 **Acknowledgements**

319 This study did not receive any external financial support.

320 **Supplementary files**

321 Figure C.1 and table C.1 can be found in Appendix C. Appendices A, B and C are available as online

322 supplementary documents.

References

323

324 1.   Vanrenterghem J, Nedergaard NJ, Robinson MA, Drust B. Training Load Monitoring in Team

325   Sports: A Novel Framework Separating Physiological and Biomechanical Load-Adaptation

326   Pathways. *Sport Med*. 2017. doi:10.1007/s40279-017-0714-2.

327 2.   Boyd LJ, Ball K, Aughey RJ. The reliability of minimaxX accelerometers for measuring

328   physical activity in australian football. *Int J Sports Physiol Perform*. 2011;6:311-321.

329 3.   Ehrmann FE, Duncan CS, Sindhusake D, Franzsen WN, Greene DA. GPS and Injury

330   Prevention in Professional Soccer. *J Strength Cond Res*. 2016;30(2):360-367.

331 4.   Page RM, Marrin K, Brogden CM, Greig M. Biomechanical and physiological response to a

332   contemporary soccer match-play simulation. *J Strength Cond Res*. 2015;29(10):2860-2866.

333 5.   Gaudino P, Iaia FM, Strudwick AJ, et al. Factors Influencing Perception of Effort (Session-

334   RPE) During Elite Soccer Training. *Int J Sports Physiol Perform*. 2015;10:860-864.

335   doi:10.1123/ijspp.2014-0518.

336 6.   Colby MJ, Dawson B, Heasman J, Rogalski B, Gabbett TJ. Accelerometer and GPS-Derived

337   Running Loads and Injury Risk in Elite Australian Footballers. *J Strength Cond Res*.

338   2014;28(8):2244-2252.

339 7.   Pavei G, Seminati E, Cazzola D, Minetti AE. On the estimation accuracy of the 3D body center

340   of mass trajectory during human locomotion: Inverse vs. forward dynamics. *Front Physiol*.

341   2017;8(MAR):1-13. doi:10.3389/fphys.2017.00129.

342 8.   Nedergaard NJ, Robinson MA, Eusterwiemann E, Drust B, Lisboa PJ, Vanrenterghem J. The

343   relationship between whole-body external loading and body-worn accelerometry during team

344   sports movement. *Int J Sports Physiol Perform*. 2017;12:18-26.

345 9.   Raper DP, Witchalls J, Philips EJ, Knight E, Drew MK, Waddington G. Use of a tibial

346   accelerometer to measure ground reaction force in running: A reliability and validity

347   comparison with force plates. *J Sci Med Sport*. 2018;21(1):84-88.

348   doi:10.1016/j.jsams.2017.06.010.

349   10.   Wundersitz DWT, Netto KJ, Aisbett B, Gastin PB. Validity of an upper-body-mounted

350   accelerometer to measure peak vertical and resultant force during running and change-of-

351   direction tasks. *Sport Biomech*. 2013;12(4):403-412. doi:10.1080/14763141.2013.811284.

352   11.   Vanrenterghem J, Gormley D, Robinson M, Lees A. Solutions for representing the whole-body

353   centre of mass in side cutting manoeuvres based on data that is typically available for lower

354   limb kinematics. *Gait Posture*. 2010;31(4):517-521. doi:10.1016/j.gaitpost.2010.02.014.

355   12.   Bezodis NE, North JS, Razavet JL. Alterations to the orientation of the ground reaction force

356   vector affect sprint acceleration performance in team sports athletes. *J Sports Sci*.

357   2017;35(18):1817-1824. doi:10.1080/02640414.2016.1239024.

358   13.   Hunter J, Marshall R, McNair P. Relationship between ground reaction force impluse and

359   kinematics of sprint-running acceleration. *J Appl Biomech*. 2005;21:31-43.

360   doi:10.1123/jab.21.1.31.

361   14.   Moore IS. Is There an Economical Running Technique? A Review of Modifiable

362   Biomechanical Factors Affecting Running Economy. *Sport Med*. 2016;0(0).

363   doi:10.1007/s40279-016-0474-4.

364   15.   Bazuelo-Ruiz B, Durá-Gil J V., Palomares N, Medina E, Llana-Belloch S. Effect of fatigue and

365   gender on kinematics and ground reaction forces variables in recreational runners. *PeerJ*.

366   2018;6:e4489. doi:10.7717/peerj.4489.

367   16.   Willy RW, Buchenic L, Rogacki K, Ackerman J, Schmidt A, Willson JD. In-field gait

368   retraining and mobile monitoring to address running biomechanics associated with tibial stress

369   fracture. *Scand J Med Sci Sports*. 2016;26(2):197-205. doi:10.1111/sms.12413.

370   17.   Loundagin LL, Schmidt T, Edwards WB. Mechanical Fatigue of Bovine Cortical Bone Using

371   Ground Reaction Force Waveforms in Running. *J Biomech Eng*. 2018;140(3):1-5.

372   doi:10.1115/1.4038288.

373   18.   Scott SH, Winter DA. Internal forces at chronic running injury sites. *Med Sci Sport Exerc*.

374   1990;22(3):357-369.

375   19.   Edwards WB. Modeling Overuse Injuries in Sport as a Mechanical Fatigue Phenomenon. *Exerc*

376   *Sport Sci Rev*. 2018;46(4):224-231. doi:10.1249/JES.0000000000000163.

377   20.   Cardinale M, Varley MC. Wearable Training-Monitoring Technology: Applications,

378   Challenges, and Opportunities. *Int J Sports Physiol Perform*. 2017;12(S2):55-62.

379   21.   Camomilla V, Bergamini E, Fantozzi S, Vannozzi G. Trends Supporting the In-Field Use of

380   Wearable Inertial Sensors for Sport Performance Evaluation: A Systematic Review. *Sensors*.

381   2018;18(3):873. doi:10.3390/s18030873.

382   22.   Chambers R, Gabbett TJ, Cole MH, Beard A. The Use of Wearable Microsensors to Quantify

383   Sport-Specific Movements. *Sport Med*. 2015;45(7):1065-1081. doi:10.1007/s40279-015-0332-

384   9.

385   23.   Dellaserra CL, Gao Y, Ransdell L. Use of integrated technology in team sports: a review of

386   opportunities, challenges, and future directions for athletes. *J Strength Cond Res*.

387   2014;28(2):556-573. doi:10.1519/JSC.0b013e3182a952fb.

388   24.   Nedergaard NJ, Robinson MA, Drust B, Lisboa PJ, Vanrenterghem J. Predicting ground

389   reaction forces from trunk kinematics: a mass-spring-damper model approach. In: *35th*

390   *Conference of the International Society of Biomechanics in Sports*. ; 2017:432-435.

391   25.   Bobbert MF, Schamhardt HC, Nigg BM. Calculation of vertical ground reaction force

392   estimates during running from positional data. *J Biomech*. 1991;24(12):1095-1105.

393   doi:10.1016/0021-9290(91)90002-5.

394   26.   Pavei G, Seminati E, Storniolo JLL, Peyré-Tartaruga LA. Estimates of running ground reaction

395   force parameters from motion analysis. *J Appl Biomech*. 2017;33(1):69-75.

396   doi:10.1123/jab.2015-0329.

397   27.   Dempster WT. Space requirements of the seated operator: Geometrical, Kinematic, and

398   Mechanical Aspects of the Body With Special Reference to the Limbs. *WADC Tech Rep*.

399   1955:55-159.

400   28.   Hanavan EP. A mathematical model of the human body. *WADC Tech Rep AMRL-TR-64-102,*

401   *Aerosp Med Researsch Lab Wright-Patterson Air Force Base, OH*. 1964.

402   29.   Hopkins WG, Marshall SW, Batterham AM, Hanin J. Progressive statistics for studies in sports

403   medicine and exercise science. *Med Sci Sports Exerc*. 2009;41(1):3-12.

404   doi:10.1249/MSS.0b013e31818cb278.

405   30.   Bland JM, Altman DG. Statistical methods for assessing agreement between two methods of

406   clinical measurement. *Int J Nurs Stud*. 2010;47(8):931-936. doi:10.1016/j.ijnurstu.2009.10.001.

407   31.   Udofa AB, Ryan LJ, Weyand PG. Impact Forces During Running: Loaded Questions, Sensible

408   Outcomes. In: *IEEE 13th International Conference on Wearable and Implantable Body Sensor*

409   *Networks (BSN)*. ; 2016:371-376.

410   32.   Vigh-Larsen JF, Dalgas U, Andersen TB. Position-Specific Acceleration and Deceleration

411   Profiles in Elite Youth and Senior Soccer Players. *J Strength Cond Res*. 2018;32(4):1114-1122.

412   doi:10.1519/JSC.0000000000001918.

413   33.   Dalen T, Jørgen I, Gertjan E, Havard HG, Ulrik W. Player load, Acceleration, and Deceleration

414   during 45 Competitive Matches of Elite Soccer. *J Strength Cond Res*. 2016;30(2):351-359.

415   34.   Datson N, Drust B, Weston M, Gregson W. Repeated high-speed running in elite female soccer

416   players during international competition. *Sci Med Footb*. 2018:1-7.

417   doi:10.1080/24733938.2018.1508880.

418   35.   Akenhead R, Hayes PR, Thompson KG, French D. Diminutions of acceleration and

419   deceleration output during professional football match play. *J Sci Med Sport*. 2013;16(6):556-

420   561. doi:10.1016/j.jsams.2012.12.005.

421   36.   Kyröläinen H, Avela J, Komi P V. Changes in muscle activity with increasing running speed. *J*

422   *Sports Sci*. 2005;23(10):1101-1109. doi:10.1080/02640410400021575.

423   37.   Harper DJ, Kiely J. Damaging nature of decelerations: Do we adequately prepare players? *BMJ*

424   *Open Sport Exerc Med*. 2018;4(e000379):1-3. doi:10.1136/bmjsem-2018-000379.

425   38.   Roetenberg D, Luinge H, Slycke P. *Xsens MVN: Full 6DOF Human Motion Tracking Using*

426   *Miniature Inertial Sensors*.; 2013. doi:10.1.1.569.9604.

427   39.   Karatsidis A, Bellusci G, Schepers MH, de Zee M, Andersen MS, Veltink PH. Estimation of

428   Ground Reaction Forces and Moments During Gait Using Only Inertial Motion Capture.

429   *Sensors*. 2017;17(75):1-22. doi:10.3390/s17010075.

430   40.   Jamkrajang P, Robinson MA, Limroongreungrat W, Vanrenterghem J. Can segmental model

431   reductions quantify whole-body balance accurately during dynamic activities? *Gait Posture*.

432   2017;56(March):37-41. doi:10.1016/j.gaitpost.2017.04.036.

433   41.   Perrott MA, Pizzari T, Cook J, McClelland JA. Comparison of lower limb and trunk

434   kinematics between markerless and marker-based motion capture systems. *Gait Posture*.

435   2017;52:57-61. doi:10.1016/j.gaitpost.2016.10.020.

436   42.   Abrams GD, Harris AHS, Andriacchi TP, Safran MR. Biomechanical analysis of three tennis

437   serve types using a markerless system. *Br J Sports Med*. 2014;48(4):339-342.

438   doi:10.1136/bjsports-2012-091371.

439   43.   Grigg J, Haakonssen E, Rathbone E, Orr R, Keogh JWL. The validity and intra-tester reliability

440   of markerless motion capture to analyse kinematics of the BMX Supercross gate start. *Sport*

441   *Biomech*. 2018;17(3):383-401. doi:10.1080/14763141.2017.1353129.

442   44.   Sperlich B, Düking P, Holmberg H-C. A SWOT Analysis of the Use and Potential Misuse of

443   Implantable Monitoring Devices by Athletes. *Front Physiol*. 2017;8(629):1-3.

444   doi:10.3389/fphys.2017.00629.

445   45.   Wouda FJ, Giuberti M, Bellusci G, et al. Estimation of Vertical Ground Reaction Forces and

446   Sagittal Knee Kinematics During Running Using Three Inertial Sensors. *Front Physiol*.

447   2018;9(March):1-14. doi:10.3389/fphys.2018.00218.

448   46.   Johnson WR, Mian A, Donnelly CJ, Lloyd D, Alderson J. Predicting athlete ground reaction

449   forces and moments from motion capture. *Med Biol Eng Comput*. 2018.

450   47.   Pogson M, Verheul J, Robinson MA, Vanrenterghem J, Lisboa PJ. Estimating mechanical load

451   in running activities: A neural network method to predict task- and step-specific ground

452   reaction forces from trunk acceleration. *Under Rev*. 2018.

453   48.   Johnson WR, Alderson J, Lloyd DG, Mian A. Predicting Athlete Ground Reaction Forces and

454   Moments from Spatio-temporal Driven CNN Models. *IEEE Trans Biomed Eng*. 2018.

455   doi:10.1109/TBME.2018.2854632.

456   49.   Lee MK, Le NS, Fang AC, Koh MTH. Measurement of body segment parameters using dual

457   energy X-ray absorptiometry and three-dimensional geometry: An application in gait analysis.

458   *J Biomech*. 2009;42(3):217-222. doi:10.1016/j.jbiomech.2008.10.036.

459   50.   Durkin JL, Dowling JJ, Andrews DM. The measurement of body segment inertial parameters

460   using dual energy X-ray absorptiometry. *J Biomech*. 2002;35:1575-1580. doi:10.1016/S0021-

461   9290(02)00227-0.

462   51.   Camomilla V, Dumas R, Cappozzo A. Human movement analysis: The soft tissue artefact

463   issue. *J Biomech*. 2017;62:1-4. doi:10.1016/j.jbiomech.2017.09.001.

464   52.   Bezodis NE, Salo AIT, Trewartha G. Excessive fluctuations in knee joint moments during early

465   stance in sprinting are caused by digital filtering procedures. *Gait Posture*. 2013;38:653-657.

466   doi:10.1016/j.gaitpost.2013.02.015.

467   53.   Robertson DGE, Dowling JJ. Design and responses of Butterworth and critically damped

468   digital filters. *J Electromyogr Kinesiol*. 2003;13(6):569-573. doi:10.1016/S1050-

469   6411(03)00080-4.

470

471   **Figure captions**

472

473   **Figure 1** Root mean square errors (RMSE) for resultant GRF curves estimated from fifteen segmental

474   accelerations. Inset: representative measured (black solid line) and estimated (red dashed line) GRF

475   profiles are shown, together with RMSE values for all acceleration (n=166), deceleration (n=161), 90°

476   cut (n=171), low- (n=157), moderate- (n=157) and high-speed running (n=141) trials.
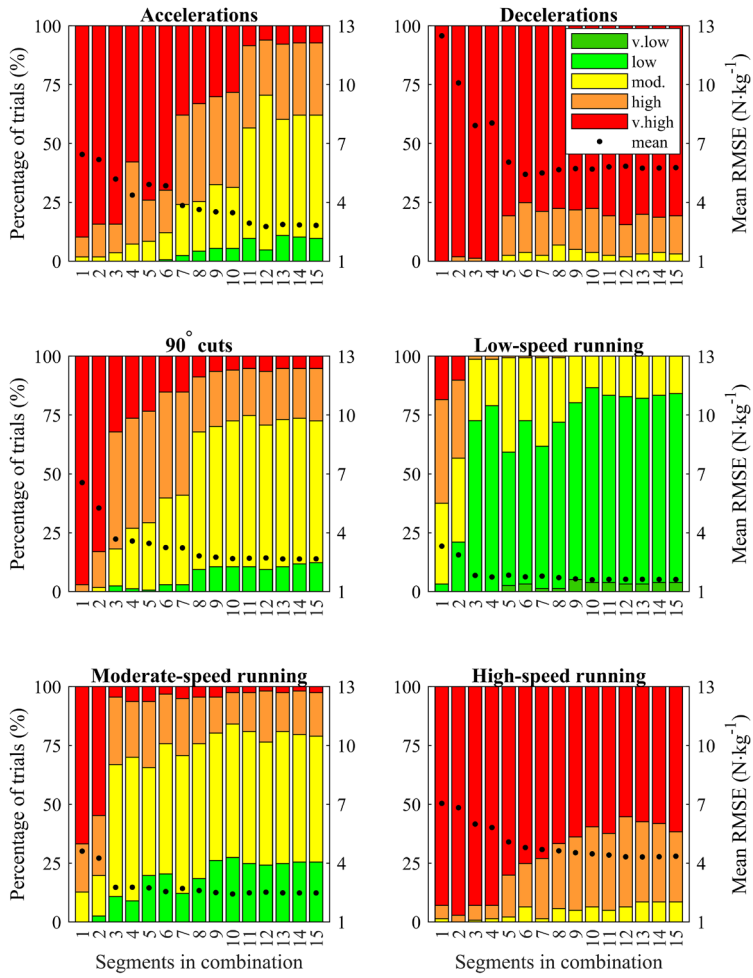
477

478   **Figure 2** Root mean square errors (RMSE) for estimated resultant GRF curves for each task. Bars

479   represent the percentage of trials (primary y-axis) within the very low (<1 N·kg^{-1}), low ($1-2$ N·kg^{-1}),

480   moderate ($2-3$ N·kg^{-1}), high ($3-4$ N·kg^{-1}) or very high (>4 N·kg^{-1}) error boundaries, and black dots

481   represent the mean errors (secondary y-axis), for each given number of segments.

482
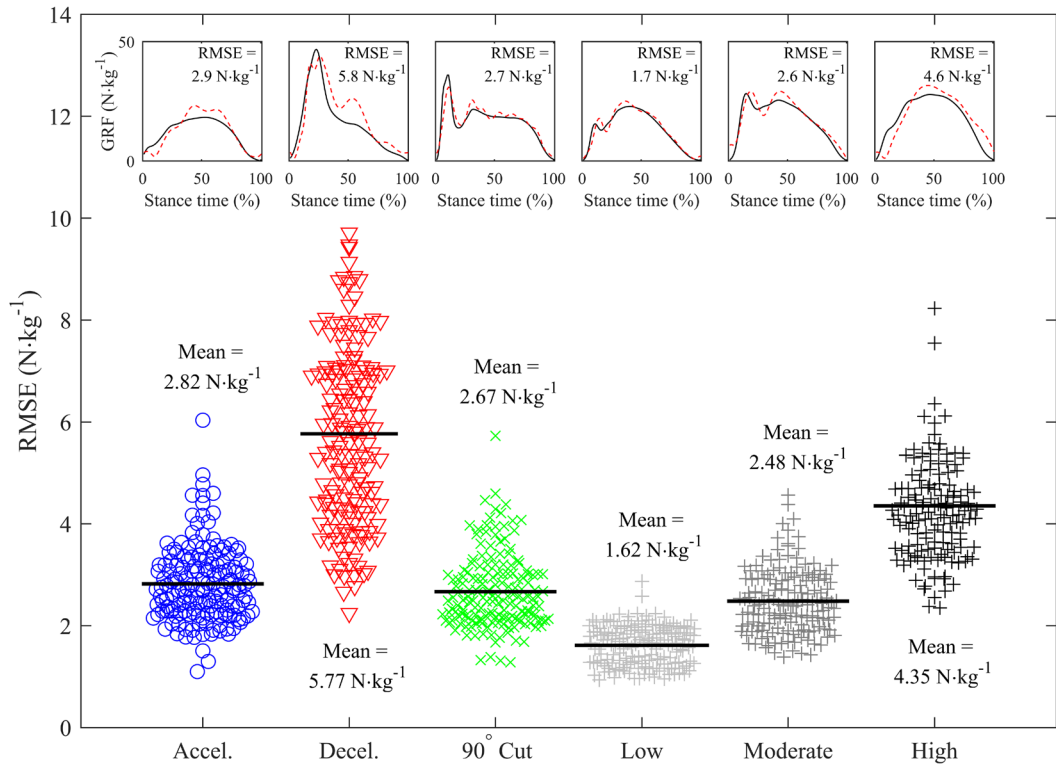
485

Table 1 Estimated resultant ground reaction force curve and loading characteristics errors

|	RMSE		Impulse error			Impact peak error			Loading rate error		
	$N \cdot kg^{-1}$	%	$N \cdot s \cdot kg^{-1}$	%	R^2	$N \cdot kg^{-1}$	%	R^2	$N \cdot kg^{-1} \cdot s^{-1}$	%	R^2
Accelerations (n=166)	2.82 ±0.7	8.4 ±14	0.25 ±0.1	9.1 ±4	0.89	3.27 ±2.8	28.5 ±33	0.21	229 ±264	33.2 ±27	0.36
Decelerations (n=161)	5.77 ±1.8	6.1 ±8.8	0.26 ±0.1	11.1 ±6	0.94	7.68 ±5.5	15 ±9	0.73	380 ±404	20.1 ±16	0.49
90° cuts (n=171)	2.67 ±0.7	3.3 ±4.1	0.21 ±0.1	3.8 ±2	0.98	3.33 ±2.9	9.8 ±8	0.75	234 ±210	24.5 ±18	0.60
Constant speed running											
Low (2-3 $m \cdot s^{-1}$; n=157)	1.62 ±0.4	1.8 ±2	0.09 ±0.06	2.3 ±2	0.96	2.22 ±2.3	13.8 ±22	0.64	173 ±101	33 ±13	0.42
Moderate (4-5 $m \cdot s^{-1}$; n=157)	2.48 ±0.6	3.1 ±5.7	0.16 ±0.1	4.6 ±2	0.93	1.96 ±1.5	9.2 ±8	0.85	281 ±174	34 ±14	0.53
High (>6 $m \cdot s^{-1}$; n=141)	4.35 ±1.3	6.4 ±7.6	0.26 ±0.2	10.4 ±12	0.77	3.52 ±3.5	11.9 ±13	0.56	661 ±419	42.8 ±21	0.12
All tasks (n=953)	3.26 ±1.7	4.8 ±8.3	0.20 ±0.1	6.8 ±7	0.99	4.00 ±4.1	13.1 ±15	0.88	323 ±326	29.3 ±19	0.68

Root mean square error (RMSE), impulse, impact peak and loading rate errors of the resultant GRF estimated from fifteen segmental accelerations, for different tasks. Values are means ± standard deviations and either absolute or relative errors compared to the measured resultant GRF. Regressions (R^2) were performed per task as well as for all trials combined.

486

487

488 **Appendix A: Marker attachment locations**

489 Full-body kinematic data in this study were collected using a seventy-six retro-reflective marker set

490 attached to anatomical landmarks of the body. The aim of this appendix is to clarify the attachment

491 locations of segment defining and segment tracking markers (figure A.1). Markers for segment

492 definition (of which some were also used for segment tracking; see figure A.1) were attached to the

493 Calcaneus, lateral Calcaneus, first and fifth Metatarsus head, lateral/medial Malleolus, lateral/medial

494 Epicondyle of the Femur, Femur greater Trochanter, anterior/posterior Superior Iliac Spine, Iliac

495 Crest, Acromion, anterior/posterior head, shoulder, lateral/medial Epicondyle of the Humerus, Styloid

496 process of the Radius and Ulna, lateral/medial Metacarpal head (all left and right), Cervical vertebrae

497 7, Thoracic vertebrae 8, and the Jugular notch and Xiphoid process of the Sternum. In addition, marker

498 clusters for segment tracking were attached to the lateral sides of the shanks and thighs (four markers

499 per cluster), as well as the forearms and upper arms (three markers per cluster).
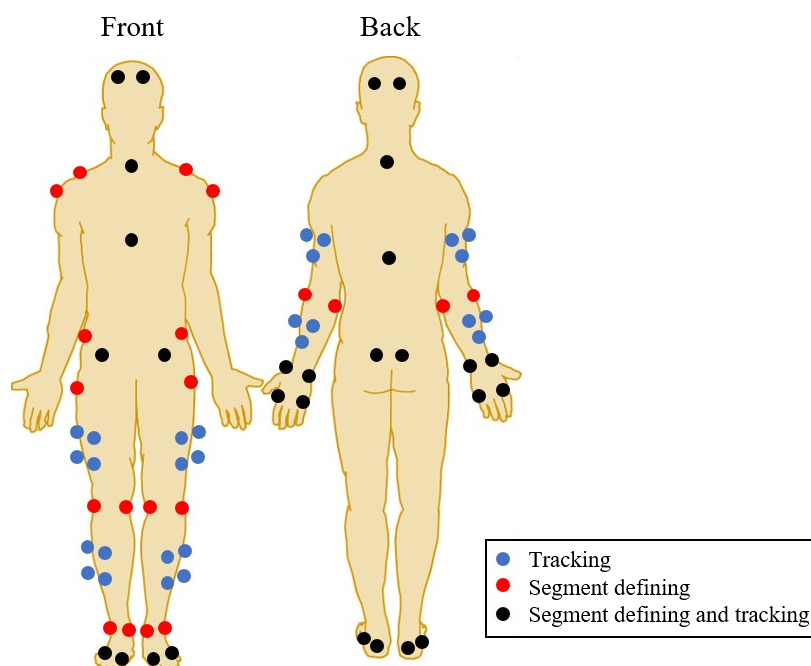
500 **Figure A.1** Attachment locations of segment tracking markers (blue), segment defining markers (red) and

501 markers used for both (black).

502

503

Appendix B: Marker trajectory filter cut-off frequencies

505 *Objective*

506 Segmental accelerations used to estimate ground reaction forces (GRFs) in this study were derived

507 from motion capture-based marker trajectories. Accuracy of estimated GRF profiles is thus dependent

508 on marker trajectory processing before calculating the segmental centre of mass (CoM) accelerations.

509 The aim of this appendix was, therefore, to investigate what filter cut-off frequency lead to the most

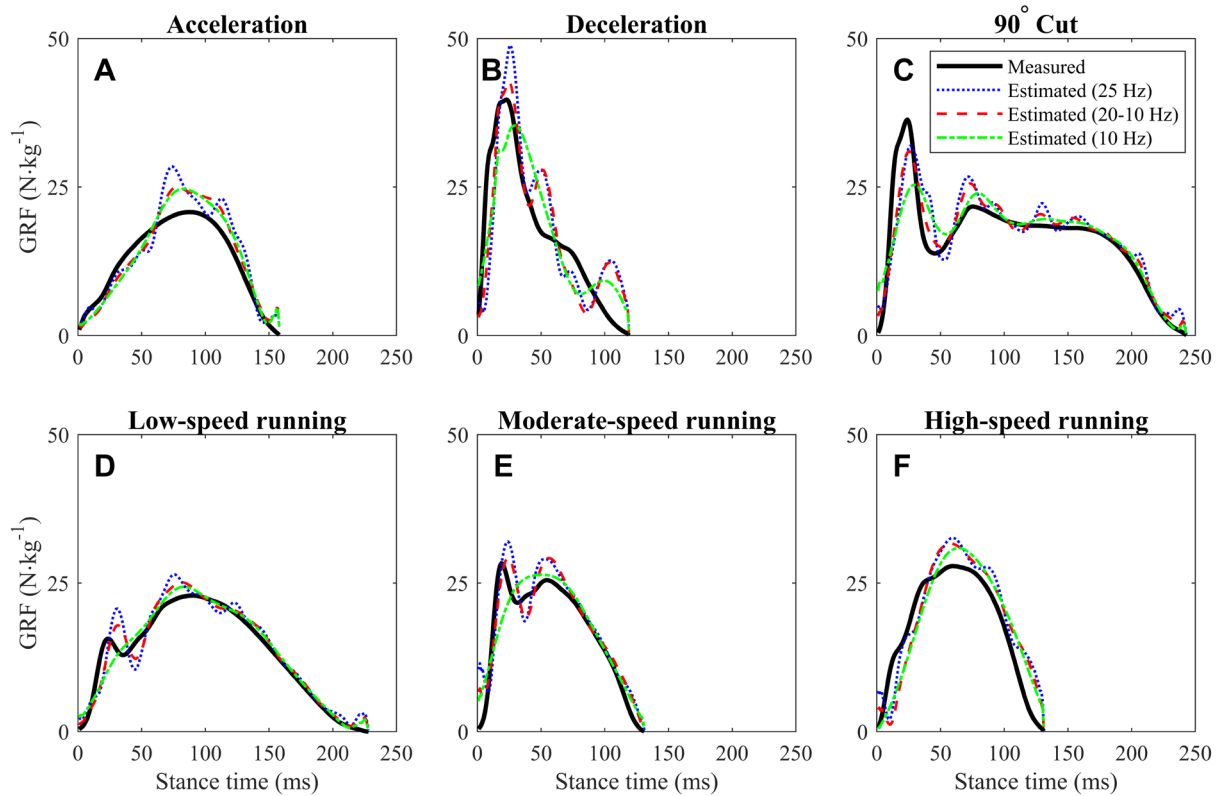510 accurate resultant GRF estimates.

511 *Methods*

512 Kinematic and kinetic data for ten subjects (7 males and 3 females, age 24±5 yrs, height 176±8 cm,

513 mass 72±9 kg) was used (see the methods section of the main paper for more detail on the data

514 collection and processing). Marker trajectories were filtered with a 2nd order Butterworth low-pass

515 filter using four different cut-off frequencies (25 Hz, 20 Hz, 15 Hz and 10 Hz), while force data were

516 filtered at 50 Hz. Visual screening of the data revealed relatively large trunk marker vibrations

517 compared to the other markers, which was likely due to marker attachment to the shirt rather than the

518 skin. Therefore, combinations of filter cut-off frequencies (20-15 Hz, 20-10 Hz and 15-10 Hz) were

519 also examined, i.e. markers defining the trunk segment were filtered at a lower cut-off frequency than

520 the other markers. Trunk defining markers that were filtered at a lower cut-off frequency were those

521 attached to the left and right Iliac Crest and Acromion, Cervical vertebrae 7, Thoracic vertebrae 8, and

522 the Jugular notch and Xiphoid process of the Sternum.

523 *Results*

524 Estimated GRF errors typically decreased for lower cut-off frequencies (table B.1). For higher

525 frequencies (25 Hz, 20 Hz) the estimated GRF profiles included more oscillations compared to the

526 lower cut-off frequencies (15 Hz, 10 Hz) (figure B.1). Consequently, RMSEs were lower across all

527 tasks when marker data were filtered at 15 Hz, compared to 25 and 20 Hz. However, only for

528 accelerations and constant speed running, errors were further reduced when a 10 Hz filter was applied,

529 while over-smoothing of estimated GRF profiles resulted in the loss of important GRF characteristics

530 (e.g. impact peak) for the other tasks (figure B.1 C, D, E). When a combination of two cut-off

531   frequencies (20-15, 20-10 and 15-10 Hz) was used, however, RMSE values were further reduced. For

532   most tasks separately, as well as all trials combined, a combination where the trunk was filtered at 10

533   Hz resulted in the most accurate GRF estimates (table B.1; figure B.1).

534   **Figure B.1** Representative examples of measured resultant ground reaction force (GRF; black solid line) profiles

535   and resultant GRF estimated from marker trajectories filtered at 25 Hz (blue dotted line), 20-10 Hz (red dashed

536   line) or 10 Hz (green dashed line), for each task.

**Table B.1** Marker trajectory filter cut-off frequency comparison

	25 Hz	20 Hz	20-15 Hz	20-10 Hz	15 Hz	15-10 Hz	10 Hz
Accelerations	3.7±1	3.4±0.9	3.1±0.8	2.8±0.7	3±0.8	2.6±0.6	2.4±0.6
Decelerations	7.7±2.4	7.4±2.3	6.8±2	6±1.8	7.3±2.2	6.4±1.9	8±2.5
90° Cuts	3.4±0.8	3.2±0.8	3±0.7	2.7±0.7	3.1±0.8	2.8±0.7	3.4±0.9
Constant speed running							
Low (2-3 m·s⁻¹)	2.3±0.6	2.1±0.6	1.9±0.5	1.7±0.4	1.9±0.5	1.6±0.4	1.7±0.5
Moderate (4-5 m·s⁻¹)	3.3±0.9	3.1±0.8	2.9±0.7	2.6±0.6	3±0.8	2.6±0.6	2.9±0.7
High (>6 m·s⁻¹)	5.4±1.3	5.1±1.3	4.8±1.2	4.4±1	4.9±1.2	4.4±1	4.7±1.3
All tasks	4.3±2.2	4.1±2.1	3.8±2	3.4±1.7	3.9±2.2	3.4±1.9	3.9±2.5

Root mean square errors (RMSE) for each (combination of) filter cut-off frequencies. Values are means ± standard deviation per task, as well as all tasks combined. The best cut-off frequency per task is highlighted in green shading.

537 *Conclusions*

538 Estimated resultant GRF profiles were more accurate across tasks when a combination of different cut-

539 off frequencies was used for different markers. More specifically, the best results were obtained when

540 marker trajectories were filtered at a 20 Hz cut-off frequency, with trunk defining markers filtered at

541 10 Hz. These cut-off frequencies were, therefore, used to filter marker trajectory data before further

542 processing.

543

Appendix C: Supplementary results
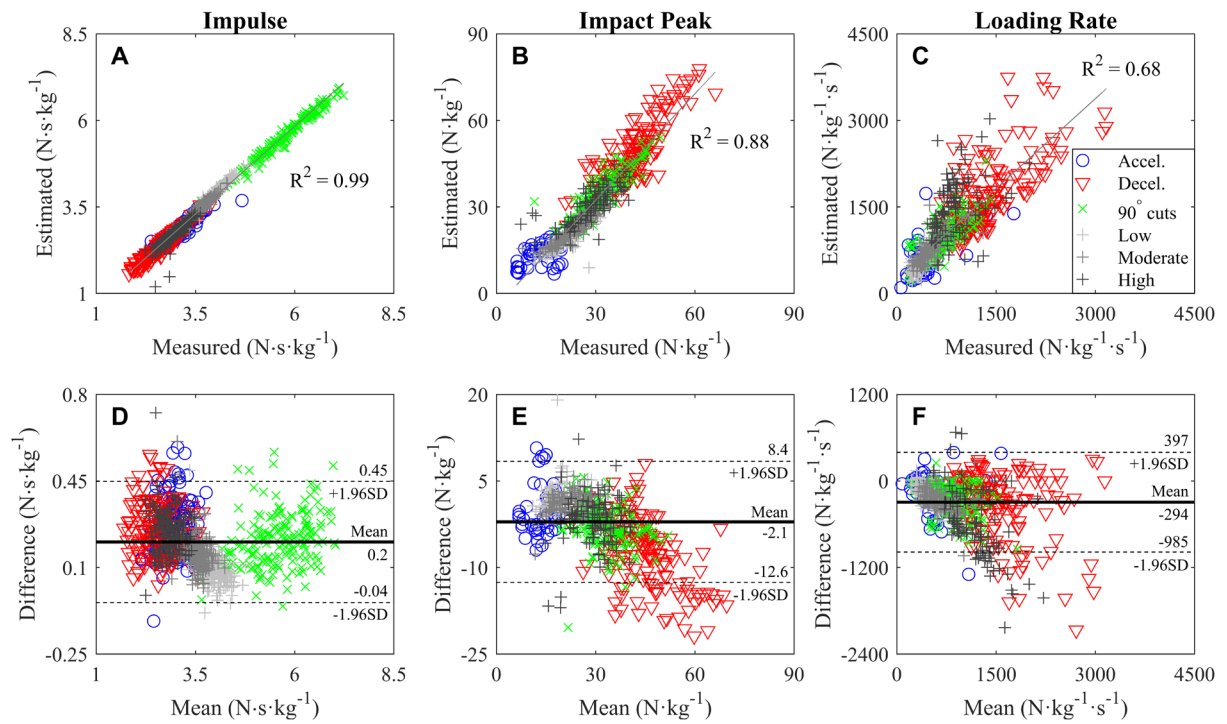
Figure C.1 Regression (A-C) and Bland-Altman (D-F) plots between measured and estimated

resultant GRF loading characteristics impulse, impact peak and loading rate.

547

Table C.1 The best combinations of segments across all tasks for each given number of segments

#	Segments in the combination	RMSE (N·kg⁻¹) Mean	SD
1	Trunk	6.76	±3.62
2	Trunk + thigh	5.91	±3.17
3	Trunk + thighs	4.54	±2.48
4	Trunk + thighs + pelvis	4.36	±2.47
5	Trunk + thighs + pelvis + head	4.00	±1.94
6	Trunk + thighs + pelvis + shanks	3.76	±1.81
7	Trunk + thighs + shanks + head + upper arm	3.61	±1.66
8	Trunk + thighs + shanks + head + upper arm + forearm	3.49	±1.73
9	Trunk + thighs + shanks + head + upper arms + forearm	3.42	±1.75
10	Trunk + thighs + shanks + head + upper arms + forearms	3.37	±1.74
11	Trunk + thighs + shanks + head + upper arms + forearms + hand	3.31	±1.73
12	Trunk + thighs + shanks + head + upper arms + forearms + hand + foot	3.28	±1.72
13	Trunk + thighs + shanks + head + upper arms + forearms + hand + feet	3.26	±1.71
14	Trunk + thighs + shanks + head + upper arms + forearms + hands + feet	3.26	±1.71
15	Trunk + thighs + shanks + head + upper arms + forearms + hands + feet + pelvis	3.26	±1.72

Best combinations of segments (i.e. with the lowest mean root mean square errors (RMSE) across subjects, tasks and trials) for each number of segments. If only one of two segments was included in a combination (e.g. thigh or foot rather than thighs or feet), this was the segment on the side of the support leg. SD = standard deviation.

548

549